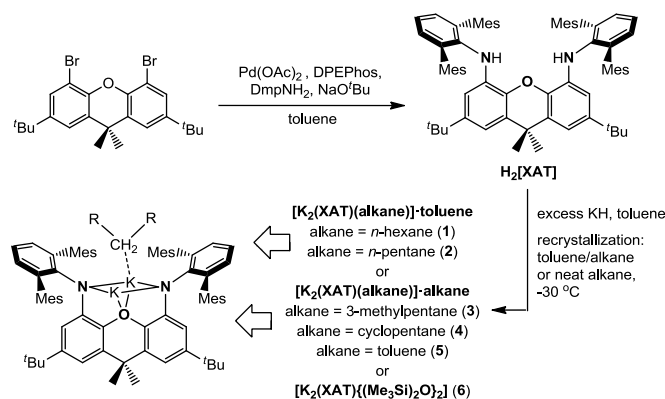


## Potassium–Alkane Interactions within a Rigid Hydrophobic Pocket\*\*

Nicholas R. Andreychuk and David J. H. Emslie\*

Metal-alkane complexes are of importance due to their involvement in alkane C–H activation reactions<sup>[1]</sup> and hydrocarbon adsorption in alkali metal-containing zeolites.<sup>[2]</sup> However, observable metal-alkane complexes are scarce as a consequence of the poor donor/acceptor character of alkanes and the low polarity of C–H bonds. Examples detected by NMR spectroscopy include [(C<sub>5</sub>R<sub>5</sub>)Re(CO)<sub>2</sub>(alkane)],<sup>[3,4]</sup> [(C<sub>5</sub>R<sub>5</sub>)M(CO)(PF<sub>3</sub>)(alkane)] (M = Re or Mn),<sup>[4]</sup> [TpRe(CO)<sub>2</sub>(alkane)],<sup>[5]</sup> [(PONOP)Rh(CH<sub>4</sub>)<sup>+</sup>] (PONOP = 2,6-(<sup>t</sup>Bu<sub>2</sub>PO)<sub>2</sub>C<sub>5</sub>H<sub>3</sub>N),<sup>[6]</sup> and [(C<sub>6</sub>Et<sub>6</sub>)W(CO)<sub>2</sub>(*n*-pentane)],<sup>[7]</sup> but none of these complexes have proven sufficiently robust to allow isolation or crystallization. At the other end of the spectrum lie crystallographically characterized metal–alkane complexes<sup>[8]</sup> which have not been observed in solution. The only members of this group are Reed's iron(II) double A-frame porphyrin–heptane complex,<sup>[9]</sup> Meyer's uranium(III)–alkane complexes,<sup>[10]</sup> and Weller's rhodium(I) norbornane complex,<sup>[11]</sup> and in all cases, the metal–alkane interaction has been considered to possess some degree of covalency, perhaps with additional stabilization from interactions between the alkane and the ligand framework. Herein we describe potassium complexes of a new highly rigid and sterically encumbered NON-donor ligand, all of which feature remarkably short intermolecular K–alkane distances in the solid state.

Palladium-catalyzed coupling of 4,5-dibromo-2,7-di-*tert*-butyl-9,9-dimethylxanthene with 2 equiv. of 2,6-dimesitylaniline afforded 4,5-bis(2,6-dimesitylanilino)-2,7-di-*tert*-butyl-9,9-dimethylxanthene (H<sub>2</sub>[XAT]; Scheme 1); an extremely sterically hindered analogue of the known 4,5-bis(2,6-diisopropylanilino)-2,7-di-*tert*-butyl-9,9-dimethylxanthene<sup>[12]</sup> and 4,5-bis(2,4,6-trimethylanilino)-2,7-di-*tert*-butyl-9,9-dimethylxanthene<sup>[13]</sup> pro-ligands. Reaction of H<sub>2</sub>[XAT] with excess KH in toluene yielded the dipotassium salt, and filtration and layering with hexanes at –30 °C deposited vibrant yellow X-ray-quality crystals of [K<sub>2</sub>(XAT)(*n*-hexane)]-toluene (**1**; Scheme 1, Figure 1). The potassium atoms in **1** are bound to bridging amido- and ether-donors forming a square pyramidal K<sub>2</sub>N<sub>2</sub>O core with oxygen in the apical site. However, an unexpected feature is close approach of a molecule of hexane to K(1), with a K(1)–C(1S) distance of 3.284(4) Å.



**Scheme 1.** Synthesis of H<sub>2</sub>[XAT] and **1-6** [Dmp = 2,6-dimesitylphenyl; Mes = mesityl; DPEPhos = bis{2-(diphenyl-phosphino)phenyl}ether].

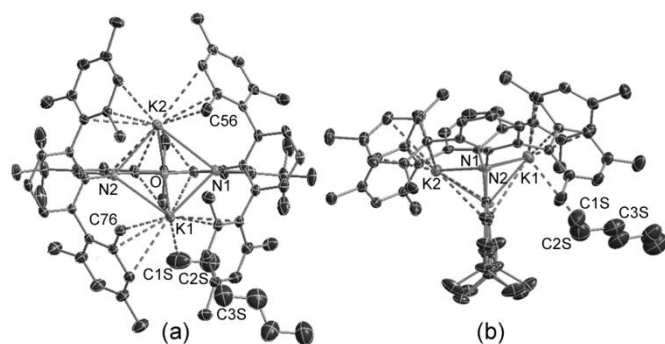


**Figure 1.** Two views of the X-ray Crystal Structure of [K<sub>2</sub>(XAT)(*n*-hexane)]-toluene (**1**). Hydrogen atoms and lattice solvent are omitted for clarity and ellipsoids are at 50 %. K–C distances less than 3.50 Å are highlighted as dotted lines.

The Fe–C distances in Reed's iron porphyrin heptane complex are 2.5 and 2.8 Å (the heptane molecule and the Fe atoms are disordered; calculated Fe–C distances for methane, ethane, propane and butane complexes are 2.68–2.70 Å),<sup>[9]</sup> the U–C distances in Meyer's uranium–alkane complexes range from 3.731(8) to 3.864(7) Å (the calculated U–C distance for the methylcyclohexane complex is 3.974 Å),<sup>[10]</sup> and the Rh–C distances in Weller's rhodium norbornane complex are 2.480(11) and 2.494(10) Å.<sup>[11]</sup> To enable a rough comparison between the M–C distances in the more ionic uranium complex and complex **1**, ionic radii for U<sup>3+</sup> and K<sup>+</sup> (1.03 and 1.38 Å for a coordination number of six)<sup>[14]</sup> may be subtracted from the crystallographic M–C distances, yielding values of 2.70–2.83 and 1.90 Å, respectively. The K–C distance in complex **1** is therefore notably short, and even falls at the lower end of the range of K–C distances observed for face-on K–benzene and K–toluene interactions; typically 3.2 to 3.5 Å.<sup>[15,16]</sup> The K–alkane interaction in **1** can be surmised to involve a weak electrostatic (primarily cation–induced dipole)<sup>[17]</sup> K–alkane interaction stabilized by interactions between the alkane and the hydrophobic ligand pocket.

An analogous intermolecular potassium–alkane interaction is not observed at K(2), perhaps as a result of crystal packing forces; the *para*-methyl carbon C(48) of a mesityl group in an adjacent

[\*] N. R. Andreychuk, Prof. D. J. H. Emslie  
Department of Chemistry, McMaster University,  
1280 Main Street West, Hamilton, ON, L8S 4M1, Canada  
Fax: (+ 1) 905-522-2509  
E-mail: emslied@mcmaster.ca  
Homepage:  
<http://www.chemistry.mcmaster.ca/emslied/emslied.html>

[\*\*] D.J.H.E. thanks NSERC of Canada for a Discovery Grant.  
N.R.A. thanks NSERC of Canada and the province of  
Ontario for CGS-M and OGS support. We are also grateful  
to H. A. Jenkins for help with X-ray crystallography, and to  
P. W. Ayers and I. Vargas-Baca for helpful discussions  
regarding DFT calculations.



Supporting information for this article is available on the  
WWW under <http://www.angewandte.org> or from the author.

[K<sub>2</sub>(XAT)(hexane)] molecule is positioned 3.538(3) Å from K(2). However, both potassium atoms in **1** are forced into close proximity with flanking mesityl groups and the xanthene backbone, leading to a large number of K–C<sub>arene</sub> and K–C<sub>methyl</sub> distances below 3.50 Å (Figure 1). In particular, the intramolecular K–C<sub>methyl</sub> distances K(2)–C(56) and K(1)–C(76) are 3.180(3) and 3.230(3) Å. For comparison, the intramolecular K–CHR<sub>3</sub> interactions in sterically encumbered [KSi(SiMe<sub>3</sub>)<sub>3</sub>]<sub>2</sub><sup>[16]</sup>, [KC(SiMe<sub>3</sub>)<sub>3</sub>]<sub>n</sub><sup>[18]</sup> and [K<sub>2</sub>(O{SiMe<sub>2</sub>C(SiHMe<sub>2</sub>)<sub>2</sub>})<sub>n</sub><sup>[19]</sup> range from 3.138(3) to 3.433(3) Å.

To further probe the disposition of the K<sub>2</sub>(XAT) moiety to interact with hydrocarbon solvent, alternative crystallization conditions were explored, yielding X-ray quality crystals of [K<sub>2</sub>(XAT)(*n*-pentane)]·toluene (**2**), [K<sub>2</sub>(XAT)(3-methylpentane)]·3-methylpentane (**3**), [K<sub>2</sub>(XAT)(cyclopentane)]·cyclopentane (**4**), [K<sub>2</sub>(XAT)(toluene)]·0.5toluene (**5**) and [K<sub>2</sub>(XAT){(Me<sub>3</sub>Si)<sub>2</sub>O}<sub>2</sub>]<sub>2</sub> (**6**) (Scheme 1 and Figure 2). The central core of structures **2-6** is analogous to that in **1** (each potassium atom is NON-coordinated and engages in intramolecular K–C interactions with surrounding mesityl groups), and in every case, one (**2-5**) or two (**6**) intermolecular K–H<sub>3</sub>CR or K–H<sub>2</sub>CR<sub>2</sub> interactions are observed. These interactions involve the 1-position of pentane and 3-methylpentane, one of the CH<sub>2</sub> groups in cyclopentane, and a methyl group of toluene and hexamethyldisiloxane, leading to K–C distances of 3.358(5) Å in **2**, 3.215(5) Å in **3**, 3.48(1) and 3.62(3) Å in **4**,<sup>[20]</sup> 3.285(7) and 3.305(9) Å in **5**, and 3.282(5) and 3.332(5) Å in **6** (bound cyclopentane in **4** and toluene in **5** are disordered over 2 positions). In **5**, toluene bridges between adjacent molecules via K–C<sub>arene</sub> interactions with distances of 3.240(7), 3.425(9) and 3.433(8) Å (Figure 2). The K–C–C angles in primary alkyl complexes **1**, **2** and **3** are 117°, 154° and 170°, the K–C<sub>methyl</sub>–C angles in **5** are 99° and 108°, and the K–C–Si angles in **6** are 171 and 176°.

Compounds **1-6** illustrate the extent to which intermolecular K–H<sub>3</sub>CR and K–H<sub>2</sub>CR<sub>2</sub> interactions are a common feature of the solid state structures of K<sub>2</sub>(XAT). However, attempts to observe alkane or O(SiMe<sub>3</sub>)<sub>2</sub> binding by <sup>1</sup>H or <sup>13</sup>C NMR in 3-methylpentane/*d*<sub>8</sub>-toluene (–80 °C), 3-methylpentane (–110 °C), cyclopentane (–80 °C), or O(SiMe<sub>3</sub>)<sub>2</sub> (–60 °C; <sup>1</sup>H NMR only) were unsuccessful, likely due to rapid exchange between free and bound solvent.

DFT calculations (ADF 2012.01, BLYP with and without Grimme's DFT-D3-BJ dispersion correction, TZ2P all-electron, gas phase, VWN, ZORA) were carried out to probe the nature of the K–alkane interaction in **3**; the complex with the shortest K–C<sub>alkane</sub> distance. Geometry optimization using the BLYP-D3-BJ functional yielded a substantially shorter K–C<sub>alkane</sub> interaction (3.218 Å) than was observed using BLYP (4.176 Å), consistent with significant stabilization of the K–alkane interaction through dispersion interactions. The calculated K–C<sub>alkane</sub> distance in **3** shows excellent agreement with the crystallographic distance [3.215(5) Å], and the three hydrogen atoms on C(1S) are located 2.82, 3.08 and 3.15 Å from K(1). The BLYP-D3-BJ functional also adequately reproduced the K–C–C angle (168.1°; cf. 170.2° in the X-ray crystal structure), the conformation of 3-methylpentane, and the K–N, K–O and intramolecular K–C distances. However, the exact position of 3-methylpentane (especially the two more remote carbon atoms), within the binding pocket deviates to some extent from that in the X-ray structure (Figure S4).

Complex **3** was investigated through a fragment approach that considered the interaction between the K<sub>2</sub>(XAT) and 3-methylpentane fragments in the geometries adopted in the calculated structure of **3**. Within this approach, the energy decomposition analysis<sup>[21]</sup> of Ziegler and Rauk<sup>[22]</sup> ( $\Delta E_{\text{int}} = \Delta E_{\text{elec}} + \Delta E_{\text{orb}} + \Delta E_{\text{disp}} + \Delta E_{\text{Pauli}}$ ; BSSE correction included) yielded a total interaction energy

( $\Delta E_{\text{int}}$ ) of –54.2 kJ mol<sup>–1</sup>, which is comprised of:  $\Delta E_{\text{elec}} = -31.6$  kJ mol<sup>–1</sup> (electrostatic interaction energy, calculated using frozen charge distributions for both fragments),  $\Delta E_{\text{orb}} = -16.6$  kJ mol<sup>–1</sup> (orbital interaction energy; this term includes all contributions resulting from intrafragment polarization),  $\Delta E_{\text{disp}} = -87.3$  kJ mol<sup>–1</sup> (dispersion interactions) and  $\Delta E_{\text{Pauli}} = 81.2$  kJ mol<sup>–1</sup> (Pauli repulsion). The total interaction energy,  $\Delta E_{\text{int}}$ , differs from the true interaction energy only by the energy needed to bring the fragments from their optimum geometries to their geometries in **3**. This preparation energy ( $\Delta E_{\text{prep}}$ ) is less than 5 % of the value of  $\Delta E_{\text{int}}$ .

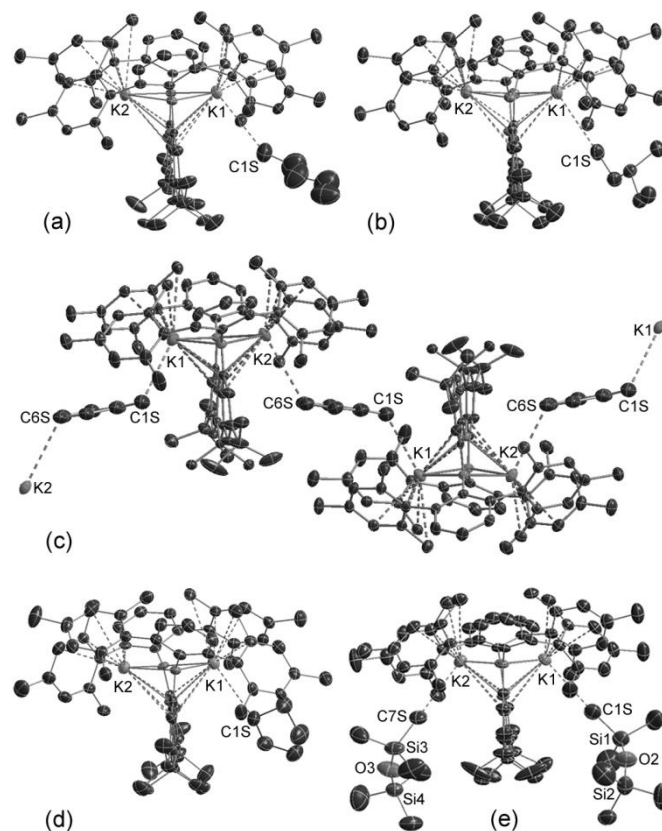


**Figure 2.** X-ray Crystal Structures of: (a) [K<sub>2</sub>(XAT)(pentane)]·toluene (**2**), (b) [K<sub>2</sub>(XAT)(3-methylpentane)]·3-methylpentane (**3**), (c) [K<sub>2</sub>(XAT)(toluene)]·0.5toluene (**5**), (d) [K<sub>2</sub>(XAT)(cyclopentane)]·cyclopentane (**4**), and (e) [K<sub>2</sub>(XAT){(Me<sub>3</sub>Si)<sub>2</sub>O}<sub>2</sub>]<sub>2</sub> (**6**). Hydrogen atoms and lattice solvent are omitted for clarity. Only one of the two orientations of cyclopentane and toluene are shown in the structures of **4** and **5**. Ellipsoids are shown at 50 % for **2-5** (collected at 100 K) and 30% for **6** (collected at 223 K). K–C distances below 3.50 Å are highlighted as dotted lines.

The closed shell interactions ( $\Delta E_{\text{disp}}$  and  $\Delta E_{\text{Pauli}}$ ) roughly cancel, leaving a net contribution of –6.0 kJ mol<sup>–1</sup>.  $\Delta E_{\text{int}}$  is therefore approximately equal to  $\Delta E_{\text{elec}} + \Delta E_{\text{orb}}$ . The SCF deformation density isosurfaces in Figure 3 highlight both the degree of polarization within the alkane fragment and the extent to which the electron density around potassium remains largely unchanged, indicating that  $\Delta E_{\text{orb}}$  is primarily due to a cation–induced dipole electrostatic interaction, rather than  $\sigma$ -donation from alkane C–H bonds to potassium. Negligible Hirshfeld charges on the K<sub>2</sub>(XAT) and alkane fragments (< ±0.003) support this interpretation.

Calculations were also performed on a simplified model for **3** (structure **3'**) in which XAT methyl and mesityl groups have been replaced by hydrogen atoms, but the coordinates of all other atoms are identical to those in the BLYP-D3-BJ/TZ2P structure of **3**. This

model lacks much of the hydrophobic pocket surrounding the metal, and fragment analysis yielded values of  $-32.3$ ,  $-15.8$ ,  $-10.7$ ,  $-36.5$  and  $30.6$   $\text{kJ mol}^{-1}$  for  $\Delta E_{\text{int}}$ ,  $\Delta E_{\text{elec}}$ ,  $\Delta E_{\text{orb}}$ ,  $\Delta E_{\text{disp}}$  and  $\Delta E_{\text{Pauli}}$ , respectively. The less negative interaction energy in **3'** highlights the importance of the hydrophobic pocket in stabilizing the K–alkane interaction. However,  $\Delta E_{\text{disp}} - \Delta E_{\text{Pauli}}$  is approximately the same in **3** and **3'**, so the more negative interaction energy for **3** can be considered to arise from more negative  $\Delta E_{\text{elec}}$  and  $\Delta E_{\text{orb}}$  contributions. Differences in  $\Delta E_{\text{elec}}$  will primarily reflect the number of electron–nucleus interactions between the alkane and the ligand framework, and the more negative  $\Delta E_{\text{orb}}$  for **3** versus **3'** implies stabilization of the polarized alkane through interactions with the surrounding pocket (image b in Figure 3 indicates polarization of the adjacent ligand framework by the polarized alkane). The ability of the hydrophobic binding pocket to stabilize the K–alkane interaction in **3** therefore extends beyond the realm of dispersion interactions.

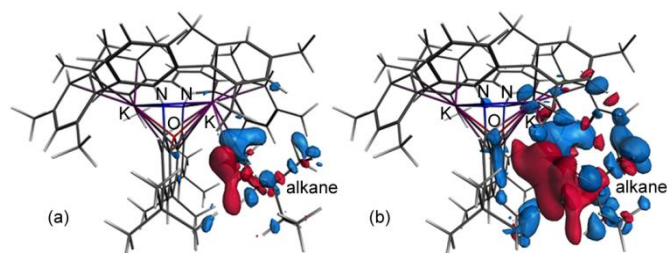


**Figure 3.** SCF deformation density isosurfaces (set to  $\pm 0.0005$  in a and  $\pm 0.0002$  in b) from fragment analysis of **3**. Blue represents increased electron density and red represents depleted electron density relative to the initial  $\text{K}_2\text{XAT}$  and 3-methylpentane fragments.

In summary, this work presents the first main group metal–alkane interactions to have been observed crystallographically, and provides a unique opportunity for computational study of well-defined K–alkane interactions. The combination of cation–induced dipole electrostatic bonding supported by interactions between the alkane and the surrounding framework is a feature common to both **3** and the K–alkane interactions proposed to occur in certain potassium-containing zeolites.<sup>[2]</sup> The effectiveness of the rigid hydrophobic binding pocket in  $\text{K}_2(\text{XAT})$  to promote and stabilize even very weak potassium–alkane interactions (as shown crystallographically in the solid state and computationally in the gas phase) also suggests that in combination with catalytically relevant metals, ligands featuring a rigid hydrophobic binding pocket may have untapped potential in alkane C–H activation chemistry.

## Experimental Section

Full experimental and characterization details for  $\text{H}_2[\text{XAT}]$  and **1–6**, and the details of DFT calculations on structures **3** and **3'** are included in the Supporting Information. CCDC 903943 (**1**), 903944 (**2**), 903945 (**5**), 903946 (**4**), 903947 (**3**) and 903948 (**6**) contain the supplementary crystallographic data for this paper. These data can be obtained free of charge from The Cambridge Crystallographic Data Centre via [www.ccdc.cam.ac.uk/data\\_request/cif](http://www.ccdc.cam.ac.uk/data_request/cif).

Received: ((will be filled in by the editorial staff))

Published online on ((will be filled in by the editorial staff))

**Keywords:** alkane complexation • potassium • noncovalent interactions • ligand design • alkali metals

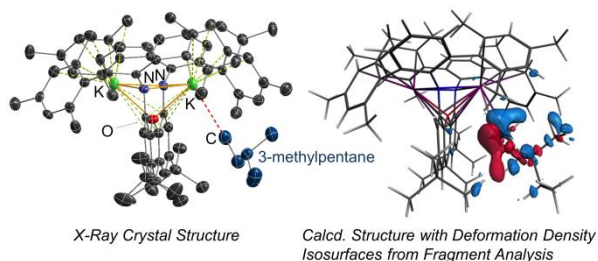
- [1] a) B. A. Arndtsen, R. G. Bergman, T. A. Mobley, T. H. Peterson, *Accounts Chem. Res.*; *Accounts Chem. Res.* **1995**, *28*, 154–162; b) J. A. Labinger, J. E. Bercaw, *Nature* **2002**, *417*, 507–514; c) R. H. Crabtree, *J. Chem. Soc. Dalton Trans.* **2001**, 2437–2450.
- [2] a) A. M. Ferrari, K. M. Neyman, S. Huber, H. Knozinger, N. Rosch, *Langmuir* **1998**, *14*, 5559–5567; b) S. Calero, D. Dubbeldam, R. Krishna, B. Smit, T. J. H. Vlucht, J. F. M. Denayer, J. A. Martens, T. L. M. Maesen, *J. Am. Chem. Soc.* **2004**, *126*, 11377–11386; c) B. Liu, B. Smit, *Phys. Chem. Chem. Phys.* **2006**, *8*, 1852–1857.
- [3] a) S. Geftakis, G. E. Ball, *J. Am. Chem. Soc.* **1998**, *120*, 9953–9954; b) J. A. Calladine, O. Torres, M. Anstey, G. E. Ball, R. G. Bergman, J. Curley, S. B. Duckett, M. W. George, A. I. Gilson, D. J. Lawes, R. N. Perutz, X. Z. Sun, K. P. C. Vollhardt, *Chemical Science* **2010**, *1*, 622–630.
- [4] G. E. Ball, C. M. Brookes, A. J. Cowan, T. A. Darwish, M. W. George, H. K. Kawanami, P. Portius, J. P. Rourke, *Proc. Natl. Acad. Sci. U. S. A.* **2007**, *104*, 6927–6932.
- [5] S. B. Duckett, M. W. George, O. S. Jina, S. L. Matthews, R. N. Perutz, X. Z. Sun, K. Q. Vuong, *Chem. Commun.* **2009**, 1401–1403.
- [6] W. H. Bernskoetter, C. K. Schauer, K. I. Goldberg, M. Brookhart, *Science* **2009**, *326*, 553–556.
- [7] R. D. Young, D. J. Lawes, A. F. Hill, G. E. Ball, *J. Am. Chem. Soc.* **2012**, *134*, 8294–8297.
- [8] The binding of ethane and propane to iron centers in an extended metal–organic framework was recently characterized by neutron diffraction: E. D. Bloch, W. L. Queen, R. Krishna, J. M. Zadrozny, C. M. Brown, J. R. Long, *Science* **2012**, *335*, 1606–1610.
- [9] D. R. Evans, T. Drovetskaya, R. Bau, C. A. Reed, P. D. W. Boyd, *J. Am. Chem. Soc.* **1997**, *119*, 3633–3634.
- [10] I. Castro-Rodriguez, H. Nakai, P. Gantzel, L. N. Zakharov, A. L. Rheingold, K. Meyer, *J. Am. Chem. Soc.* **2003**, *125*, 15734–15735.
- [11] S. D. Pike, A. L. Thompson, A. G. Algarra, D. C. Apperley, S. A. Macgregor, A. S. Weller, *Science* **2012**, *337*, 1648–1651.
- [12] C. A. Cruz, D. J. H. Emslie, L. E. Harrington, J. F. Britten, C. M. Robertson, *Organometallics* **2007**, *26*, 692–701.
- [13] R. M. Porter, A. A. Danopoulos, *Polyhedron* **2006**, *25*, 859–863.
- [14] R. D. Shannon, *Acta Cryst.* **1976**, *A32*, 751–767.
- [15] a) J. Hao, H. Song, C. Cui, *Organometallics* **2009**, *28*, 3100–3104; b) M. Niemeyer, *Inorg. Chem.* **2006**, *45*, 9085–9095; c) P. B. Hitchcock, M. F. Lappert, R. Sablong, *Dalton Trans.* **2006**, 4146–4154; d) W. J. Evans, D. B. Rego, J. W. Ziller, *Inorg. Chem.* **2006**, *45*, 3437–3443; e) G. C. Forbes, A. R. Kennedy, R. E. Mulvey, B. A. Roberts, R. B. Rowlings, *Organometallics* **2002**, *21*, 5115–5121; f) G. Bai, H. W. Roesky, M. Noltemeyer, H.-G. Schmidt, *J. Chem. Soc. Dalton Trans.* **2002**, 2437–2440; g) C. J. Schaverien, J. B. Vanmechelen, *Organometallics* **1991**, *10*, 1704–1709; h) G. R. Fuentes, P. S. Coan, W. E. Streib, K. G. Caulton, *Polyhedron* **1991**, *10*, 2371–2375.
- [16] K. W. Klinkhammer, *Chem. Eur. J.* **1997**, *3*, 1418–1431.
- [17] a) E. V. Anslin, D. A. Dougherty, *Modern physical organic chemistry*, University Science Books, Sausalito, California, **2006**; b) A. W. Ehlers, C. G. de Koster, R. J. Meier, K. Lammertsma, *J. Phys. Chem. A* **2001**, *105*, 8691–8695.
- [18] C. Eaborn, P. B. Hitchcock, K. Izod, A. J. Jaggard, J. D. Smith, *Organometallics* **1994**, *13*, 753–754.
- [19] L. J. Bowman, K. Izod, W. Clegg, R. W. Harrington, J. D. Smith, C. Eaborn, *Dalton Trans.* **2006**, 502–508.
- [20] The K–C distances in **4** should be viewed with some caution since bound cyclopentane is disordered over two positions and restraints had to be applied to ensure reasonable C–C bond distances (DFIX was used to set all five C–C distances to 1.41 Å with an ESD of 0.01 Å).
- [21] F. M. Bickelhaupt, E. J. Baerends, in *Reviews in Computational Chemistry*, Vol. 15 (Eds: K. B. Lipkowitz, D. B. Boyd), Wiley-VCH, New York, **2000**, pp. 1–86.
- [22] a) T. Ziegler, A. Rauk, *Inorg. Chem.* **1979**, *18*, 1755–1759; b) T. Ziegler, A. Rauk, *Inorg. Chem.* **1979**, *18*, 1558–1565.

Layout 2:

## Alkane Complexation

Nicholas R. Andreychuk, David J. H. Emslie\* \_\_\_\_\_ Page – Page

### Potassium–Alkane Interactions within a Rigid Hydrophobic Pocket



Potassium complexes of an extremely rigid and sterically encumbered NON-donor ligand have been prepared, and crystallization from alkane solvents yielded solid state structures featuring remarkably short potassium–alkane distances. DFT calculations highlight the presence of an electrostatic cation–induced dipole K–alkane interaction supported by interactions between the alkane and the surrounding ligand framework.

\* *Note: The suggested catch phrase brings together the ideas of alkane complexation and potassium (K).*